

Model non-Hermitian topological operators without skin effect

Daniel J. Salib,^{1,*} Sanjib Kumar Das,^{1,*} and Bitan Roy^{1,†}

¹*Department of Physics, Lehigh University, Bethlehem, Pennsylvania, 18015, USA*

We propose a general principle of constructing non-Hermitian (NH) operators for insulating and gapless topological phases in any dimension (d) that over an extended NH parameter regime feature real eigenvalues and zero-energy topological boundary modes, when in particular their Hermitian cousins are also topological. However, the topological zero modes disappear when the NH operators accommodate complex eigenvalues. These systems are always devoid of NH skin effects, thereby extending the realm of the bulk-boundary correspondence to NH systems in terms of solely the left or right zero-energy boundary localized eigenmodes. We showcase these general and robust outcomes for NH topological insulators in $d = 1, 2$ and 3 , encompassing their higher-order incarnations, as well as for NH topological Dirac, Weyl and nodal-loop semimetals. Possible realizations of proposed NH topological phases in designer materials, optical lattices and classical metamaterials are highlighted.

Introduction. Nontrivial topology and geometry of electronic wavefunctions in the bulk of quantum crystals leave signatures at the boundaries (edges, surfaces, hinges and corners) in terms of robust gapless modes therein: a phenomenon known as the bulk-boundary correspondence (BBC). It plays a prominent role in the identification of topological crystals in nature and is germane for topological insulators (TIs) [1–12], topological semimetals (TSMs) [13–18], and topological superconductors [19–23]. Broadly topological phases can be classified according to the co-dimension (d_c) of the associated boundary modes, where $d_c = d - d_B$ and d (d_B) is the dimensionality of the system (boundary modes). Thus an n th order topological phase hosts boundary modes of $d_c = n$. For example, three-dimensional topological crystals supporting surface ($d_B = 2$), hinge ($d_B = 1$) and corner ($d_B = 0$) modes are tagged as first-, second- and third-order topological phases, respectively [24–36].

An attempt to extend the realm of these topological phases to open quantum materials leads to non-Hermitian (NH) operators, although their exact connection with the system-to-environment interactions thus far remains illusive. Nevertheless, desired NH operators, if simple, can in principle be engineered on optical lattices [37] and in classical metamaterials [38–50]. Typically, the NH operators display NH skin effect: an accumulation of all the left and right eigenvectors at the opposite ends of a system with open boundary conditions [51–76]. Naturally, it masks the BBC in terms of left or right eigenmodes, which nonetheless is captured by their bi-orthogonal product [61], even though its direct experimental measurement remains challenging. Therefore, construction of NH topological operators, featuring BBC in terms of their left or right eigenvectors and thus devoid of the NH skin effect, is of pressing and urgent theoretical and more crucially, experimental importance.

Here, we outline a general principle of constructing such NH operators for TIs and TSMs in any dimension as an extension of their Hermitian counterparts, which we explicitly exemplify for systems of dimensionality $d \leq 3$. We show that the NH operators display the BBC in terms

of robust zero-energy boundary modes, when all its eigenvalues are purely real. But, the system becomes trivial when the eigenvalues are complex. See Figs. 1-5.

Topological models. Our construction of NH topological operators is greatly facilitated by reviewing the universal model Bloch Hamiltonian for d -dimensional Hermitian topological phases, which can be decomposed as

$$H_{\text{Her}}(\mathbf{k}) = H_{\text{Dir}}(\mathbf{k}) + H_{\text{Wil}}(\mathbf{k}) + H_{\text{HOT}}(\mathbf{k}). \quad (1)$$

The lattice regularized Dirac kinetic energy stems from the nearest-neighbor (NN) hopping of amplitude t between orbitals of opposite parities, and it is given by

$$H_{\text{Dir}}(\mathbf{k}) = t \sum_{j=1}^d \sin(k_j a) \Gamma_j, \quad (2)$$

where a is the lattice constant in a d -dimensional hypercubic lattice, momentum $\mathbf{k} = (k_1, \dots, k_d)$, and k_1, k_2 and k_3 should be identified as k_x, k_y and k_z , respectively, for example. All the Hermitian Γ matrices appearing in this work satisfy the anticommuting Clifford algebra $\{\Gamma_j, \Gamma_l\} = \delta_{jl}$ for any j and l . Their dimensionality, explicit representations and the internal structure of the associated Dirac spinor (Ψ) depend on the microscopic details, which we reveal while discussing specific models.

The (first-order) Wilson mass, preserving all the non-spatial and crystal symmetries, and thus transforming under the trivial singlet A_{1g} representation of any crystallographic point group, is $H_{\text{Wil}}(\mathbf{k}) = \Gamma_{d+1} m(\mathbf{k})$, where

$$m(\mathbf{k}) = \Delta_1 - 2B \left[d - \sum_{j=1}^d \cos(k_j a) \right] + \sum_{s=1}^p t_s \cos(k_{d+s} a). \quad (3)$$

For now we switch off the symmetry preserving out of d -dimensional hyperplane hopping processes by setting $t_s = 0$ for all s . Then the first-order Wilson mass features band inversion within the parameter regime $0 < \Delta_1/B < 4d$, where $H_{\text{Her}}^{\text{Ins}}(\mathbf{k}) = H_{\text{Dir}}(\mathbf{k}) + H_{\text{Wil}}(\mathbf{k})$ describes a d -dimensional first-order TI, hosting zero-energy gapless boundary modes of $d_c = 1$. Prominent examples are end

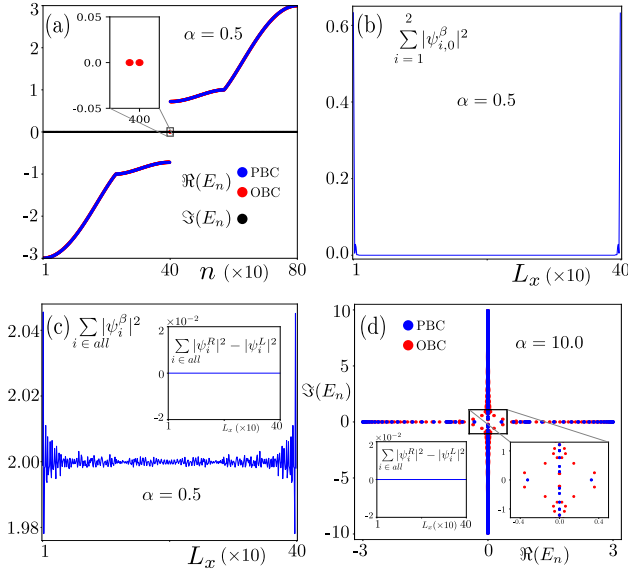


FIG. 1. Non-Hermitian Su-Schrieffer-Heeger model. (a) Eigenvalue spectrum for $\alpha = 0.5$ with a periodic boundary condition (PBC) and an open boundary condition (OBC), showing their reality condition and the existence of two near zero-energy topological modes (inset) for $|\alpha| < 1$. (b) Amplitude square of the right ($\beta = R$) or left ($\beta = L$) eigenvectors of two zero-energy modes, showing their sharp localization near the ends of the chain. (c) The same as (b), but for all the right or left eigenvectors, showing no left-right asymmetry and confirming the absence of any NH skin effect (inset). (d) Eigenvalues for $\alpha = 10$, showing its generic complex nature, the absence of any zero-energy topological modes and skin effect for $|\alpha| > 1$. Here, we set $t = B = 1$ and $\Delta_1 = 1$.

modes of the Su-Schrieffer-Heeger insulator [77–79], edge modes of quantum anomalous [80] and spin Hall [5, 6] insulators, and surface states of three-dimensional strong Z_2 TIs [7–10]. Notice that $H_{\text{Dir}}(\mathbf{k})$ and thus $H_{\text{Her}}^{\text{Ins}}(\mathbf{k})$ also transform under the A_{1g} representation.

A hierarchy of higher-order TIs is generated by the discrete symmetry breaking Wilson masses [34, 36]

$$H_{\text{HOT}}(\mathbf{k}) = \Delta_2 \Gamma_{d+2} d_{x^2-y^2}(\mathbf{k}) + \Delta_3 \Gamma_{d+3} d_{3z^2-r^2}(\mathbf{k}), \quad (4)$$

where $d_{x^2-y^2}(\mathbf{k}) = \cos(k_1 a) - \cos(k_2 a)$ and $d_{3z^2-r^2}(\mathbf{k}) = 2 \cos(k_3 a) - \cos(k_1 a) - \cos(k_2 a)$. The term proportional to Δ_2 (Δ_3) is pertinent only for $d \geq 2$ ($d \geq 3$). While $d_{x^2-y^2}(\mathbf{k})$ transforms under the singlet B_{1g} representation of the tetragonal point group (D_{4h}) in $d = 2$, $d_{x^2-y^2}(\mathbf{k})$ and $d_{3z^2-r^2}(\mathbf{k})$ transform under the doublet E_g representation of the cubic point group (O_h) in $d = 3$. By virtue of the anticommutation relation among all the Γ matrices appearing in $H_{\text{Her}}(\mathbf{k})$, $H_{\text{HOT}}(\mathbf{k})$ acts as a mass for the gapless boundary modes of the first-order TIs in $d > 1$, and partially gaps them out, thereby yielding boundary modes with $d_c > 1$ and higher-order TIs.

As such, a finite Δ_2 converts a parent first-order TI into a second-order TI. Specifically, in $d = 2$ it

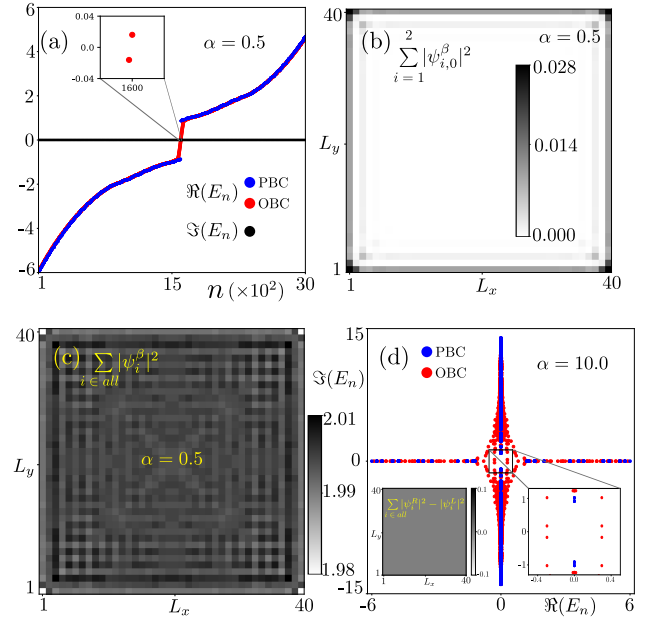


FIG. 2. Non-Hermitian Qi-Wu-Zhang model. (a) Eigenvalues for $\alpha = 0.5$ with PBCs and OBCs, confirming their reality condition and the existence of topological edge modes (inset) for $|\alpha| < 1$. (b) Amplitude square of the right ($\beta = R$) or left ($\beta = L$) eigenvectors of two closest to zero energy modes, showing their sharp edge localization. (c) The same as (b), but for all the right or left eigenvectors, showing no left-right or top-bottom asymmetry about the center of the system, thus no NH skin effect. (d) Complex eigenvalues for $\alpha = 10$, showing absence of any zero energy topological mode and NH skin effect for $|\alpha| > 1$. Here, we set $t = B = 1$ and $\Delta_1 = 6$.

hosts four zero energy modes localized at the corners in the body diagonal directions ($k_1 = \pm k_2$) along which $d_{x^2-y^2}(\mathbf{k})$ vanishes [34]. But, in $d = 3$ it features four z -directional hinge modes and gapless surface states on the top and bottom xy planes of a cubic crystal, exactly where $d_{x^2-y^2}(\mathbf{k})$ vanishes [28]. Subsequently, a finite Δ_2 and Δ_3 produce a third-order TI in $d = 3$, supporting zero modes at eight corners of a cubic crystal, placed on its body diagonals ($k_1 = \pm k_2 = \pm k_3$), only along which both $d_{x^2-y^2}(\mathbf{k})$ and $d_{3z^2-r^2}(\mathbf{k})$ vanish simultaneously [36]. One can continue this construction in $d \geq 3$ to realize the hierarchy higher-order TIs therein. However, we restrict ourselves to $d \leq 3$.

Finally, we consider the terms proportional to t_s [Eq. (3)], yielding $(d + p)$ -dimensional weak topological phases by stacking d -dimensional n th order TIs. Depending on the parameter values (Δ_1/B and t_s/B), the weak topological phase can be either gapless (known as TSMS) or insulating (trivial or weak TI). Their gapless boundary modes appear only along the stacking direction, obtained by placing the zero-energy modes of the parent n th order TI in that direction. Some well known examples are the Fermi arcs of Dirac and Weyl

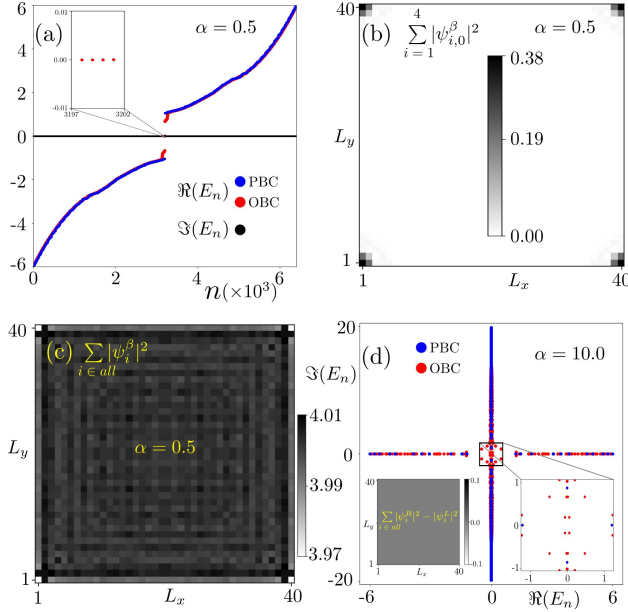


FIG. 3. Non-Hermitian second-order topological insulator in $d = 2$. (a) Real eigenvalue spectrum with PBCs and OBCs, accommodating four near zero-energy topological modes (inset) for $\alpha = 0.5$. (b) Amplitude square of the right ($\beta = R$) or left ($\beta = L$) eigenvectors of four closest to zero-energy modes, showing their sharp corner localization. (c) Same as (b), but for all the right or left eigenvectors, showing no left-right or top-bottom asymmetry about the center of the system (no NH skin effect). (d) Generic complex eigenvalues, and the absence of zero-energy topological modes and NH skin effect for $\alpha = 10$. Here, we set $t = B = 1$, $\Delta_1 = 6$ and $\Delta_2 = 1$.

semimetals [13–16, 81], drumhead surface states of nodal-loop semimetals [82–84] and hinge modes of higher-order Dirac semimetals [34, 85–87], which we will discuss in the context of NH TSMs. In this work, we focus on TSMs, although our results apply equally well for weak TIs.

NH operators. The stage is now set to construct the desired NH topological operators. The key observation is that the first-order Wilson mass matrix Γ_{d+1} anticommutes with $H_{\text{Dir}}(\mathbf{k})$ and $H_{\text{HOT}}(\mathbf{k})$. So, the products $\Gamma_{d+1}H_{\text{Dir}}(\mathbf{k})$ and $\Gamma_{d+1}H_{\text{HOT}}(\mathbf{k})$ are *anti-Hermitian*, as $(\Gamma_{d+1}\Gamma_j)^\dagger = -\Gamma_{d+1}\Gamma_j$ for $j = 1, \dots, d, d+2, d+3$. We therefore define a NH generalization of all the topological phases in terms of the NH operator

$$H_{\text{NH}}(\mathbf{k}) = H_{\text{Her}}(\mathbf{k}) + \alpha \Gamma_{d+1} [H_{\text{Dir}}(\mathbf{k}) + H_{\text{HOT}}(\mathbf{k})]. \quad (5)$$

The parameter α quantifies the strength of the non-Hermiticity. Since all the matrices in $H_{\text{NH}}(\mathbf{k})$ are mutually anticommuting, its eigenvalues are $\pm E_{\text{NH}}(\mathbf{k})$, where

$$E_{\text{NH}}(\mathbf{k}) = \left[(1 - \alpha^2) \left\{ t^2 \sum_{i=1}^d \sin^2(k_j a) + \Delta_2^2 d_{x^2-y^2}^2(\mathbf{k}) + \Delta_3^2 d_{3z^2-r^2}^2(\mathbf{k}) \right\} + m^2(\mathbf{k}) \right]^{1/2}. \quad (6)$$

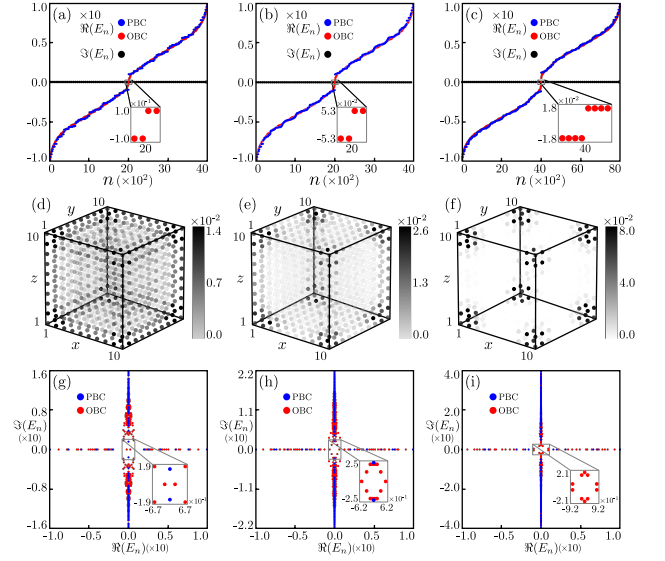


FIG. 4. Hierarchy of non-Hermitian topological insulators in $d = 3$. Real eigenvalue spectrum for $\alpha = 0.5$ with PBCs and OBCs, showing the existence of near zero-energy topological modes (insets) for (a) first-order, (b) second-order and (c) third-order TIs. Amplitude square of the right or left eigenvectors of near zero-energy modes, showing sharp localization (d) on six surfaces, (e) on four z -directional hinges and two xy surfaces, and (f) at eight corners. Panels (g)-(i) are same as (a)-(c), respectively, but for $\alpha = 10$, showing complex eigenvalue spectrum and the absence of near zero-energy modes. Here, we set $t = B = 1$, $\Delta_1 = 10$, $\Delta_2 = 1$ and $\Delta_3 = 1$.

For $\alpha = 0$, we recover the energy spectra of the Hermitian systems. For $|\alpha| < 1$ all the eigenvalues are purely real, showing a line gap. For $|\alpha| > 1$ they are complex in general with a point gap. These outcomes are insensitive to the real space boundary condition. The NH operator $H_{\text{NH}}(\mathbf{k})$ also meets some non-spatial symmetries [63, 65, 73]. If $H_{\text{Her}}(\mathbf{k})$ preserves the time-reversal (\mathcal{T}) and particle-hole (\mathcal{C}) symmetries [11], then $\mathcal{T}H_{\text{NH}}^*(\mathbf{k})\mathcal{T}^{-1} = H_{\text{NH}}(-\mathbf{k})$ and $\mathcal{C}H_{\text{NH}}^\dagger(\mathbf{k})\mathcal{T}^{-1} = -H_{\text{NH}}(-\mathbf{k})$. But, $H_{\text{NH}}(\mathbf{k})$ lacks the sublattice and pseudo-Hermiticity symmetries, by construction.

Most importantly, as Γ_{d+1} transforms under the A_{1g} representation, $\Gamma_{d+1}H_{\text{Dir}}(\mathbf{k})$ and $\Gamma_{d+1}H_{\text{HOT}}(\mathbf{k})$ preserve all the spatial symmetries of the Hermitian system and do not break any new crystal symmetry that has not been already broken in the Hermitian limit. Therefore, the eigenmodes of $H_{\text{NH}}(\mathbf{k})$ do not show any NH skin effect, by construction. Furthermore, as the anti-Hermitian component of $H_{\text{NH}}(\mathbf{k})$ and the Hermitian operator $H_{\text{Dir}}(\mathbf{k}) + H_{\text{HOT}}(\mathbf{k})$ vanish exactly at the same high symmetry time-reversal invariant momentum (TRIM) points in the Brillouin zone, the topological bound states (when present) are always pinned at zero energy, as in the Hermitian systems. Finally, we show that such topological zero-energy bound states exist only for $0 < \Delta_1/B < 4d$

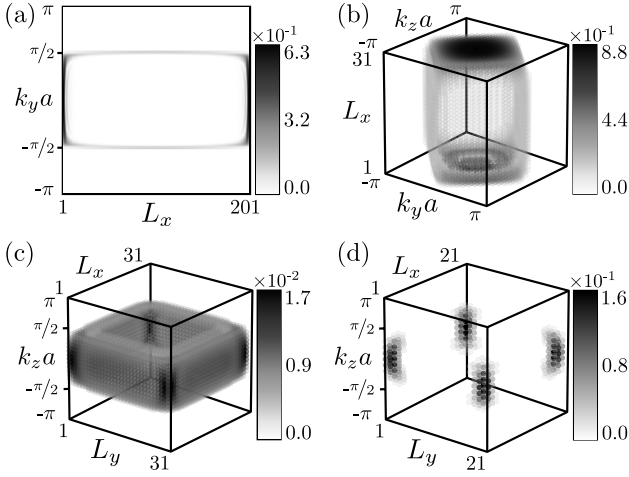


FIG. 5. Non-Hermitian topological semimetals. Boundary modes of (a) a two-dimensional NH Dirac semimetal, featuring Fermi arcs between two Dirac points at $k_y = \pm\pi/(2a)$ for $\Delta_1 = 0$ and $t_2 = B = 1$, (b) a three-dimensional NH nodal-loop semimetal, showing drumhead surface states for $\Delta_1 = 0$ and $t_2 = t_3 = B = 1$, images of the bulk nodal ring determined by $\cos(k_y a) + \cos(k_z a) = 0$, (c) a three-dimensional NH Weyl semimetal, displaying Fermi arcs in between the Weyl nodes at $k_z = \pm\pi/(2a)$, for $\Delta_1 = 0$ and $t_3 = B = 1$, and (d) a three-dimensional NH second-order Dirac semimetal with hinge Fermi arcs between two Dirac points at $k_z = \pm\pi/(2a)$ for $\Delta_1 = 0$ and $\Delta_2 = t_3 = B = 1$. Here, we set $\alpha = 0.5$.

and $|\alpha| < 1$, when the eigenvalues of $H_{\text{NH}}(\mathbf{k})$ are purely real. Next, we anchor these general outcomes for various paradigmatic models for topological phases of matter in one, two, and three dimensions.

One dimension. A NH Su-Schrieffer-Heeger model [77–79] in one dimension can be defined by taking $\Gamma_1 = \tau_1$ and $\Gamma_2 = \tau_2$. The Pauli matrices τ operates on the orbital degrees of freedom. The results are shown in Fig. 1. Analytical solutions of the topological modes can be obtained by considering a hard-wall boundary at $x = 0$ such that $\Psi_0^R(x = 0) = 0$ in a semi-infinite system occupying the region $x \geq 0$, thus $\Psi_0^R(x \rightarrow \infty) = 0$. Here, the superscript ‘R’ denotes right eigenvector. Such a mode can only be found at zero energy, explicitly given by

$$\Psi_0^R(x) = A \left(\frac{1}{t\lambda_+ + \Delta_1 + B\lambda_+^2} \right) \sum_{\delta=\pm} [\delta \exp(-\lambda_\delta x)], \quad (7)$$

where A is the overall normalization constant, and

$$\lambda_\delta = \frac{t}{2B} \sqrt{1 - \alpha^2} + \delta \sqrt{\frac{t^2}{4B^2} (1 - \alpha^2) - \frac{\Delta_1}{B}}. \quad (8)$$

Hence, zero-energy topological bound state can only be found if $|\alpha| < 1$, for which $\Re(\lambda_\delta) > 0$. As $\alpha \rightarrow 1$, such a mode becomes more delocalized. At $\alpha = 1$, the modes living on two opposite ends of the one-dimensional chain hybridize, and they disappear for $|\alpha| > 1$.

The topological modes for the first-order TIs in $d > 1$ are obtained as the zero-energy bound states with a hard-wall boundary condition in a direction along which the translational symmetry is broken, following the steps outlined above. Subsequently, their dispersive nature is revealed by computing the matrix elements of the remaining part of the Hamiltonian, with conserved momentum in the orthogonal direction(s), within the subspace of the zero modes [12]. In higher-order TIs, topological modes of reduced dimensionality are realized by partially gapping the ones for the first-order TIs by the discrete symmetry breaking Wilson mass(es). This procedure applies to all the NH TIs within our construction. Hence, the above exercise proves that topological modes in NH TIs of any order in any dimension can only be found at zero energy and when $|\alpha| < 1$. So, we only provide its numerical evidence for all the remaining cases.

Two dimensions. A NH generalization of the Qi-Wu-Zhang model [80], describing NH Chern insulators, is realized for $\Gamma_j = \tau_j$ for $j = 1, 2, 3$. The results are shown in Fig. 2. Within the topological regime, this model hosts chiral edge modes. A NH version of the Bernevig-Hughes-Zhang model [6] for a NH quantum spin Hall insulator is realized for $\Gamma_j = \sigma_3 \tau_j$ for $j = 1, 2, 3$. The Pauli matrices σ act on the spin indices. All the results are identical to those for the NH Chern insulator, except each mode now enjoys two-fold Kramers degeneracy. So, we do not show them here. Within the topological regime, this model sustains counter-propagating helical edge modes for opposite spin projections. A NH second-order TI, featuring four zero-energy corner modes [24, 34], can be realized with the addition of the Δ_2 term, accompanied by the matrix $\Gamma_4 = \sigma_1 \tau_0$, to the NH quantum spin Hall insulator model. The results are shown in Fig. 3.

Three dimensions. A three-dimensional NH first-order TI, supporting surface states on all six surfaces of a cubic crystal, is obtained with $\Gamma_j = \sigma_3 \tau_j$ for $j = 1, 2, 3$ and $\Gamma_4 = \sigma_1 \tau_0$. A NH second-order TI, supporting four z -directions hinge and xy surface modes, is realized when Δ_2 , accompanied by $\Gamma_5 = \sigma_2 \tau_0$, is finite. A three-dimensional NH third-order TI is realized when both the terms proportional to Δ_2 and Δ_3 are finite. As now $H_{\text{Her}}(\mathbf{k})$ involves six mutually anticommuting Hermitian Γ matrices, their minimal dimensionality is eight [36, 88]. We choose $\Gamma_j = \eta_3 \sigma_3 \tau_j$ for $j = 1, 2, 3$, $\Gamma_4 = \eta_3 \sigma_1 \tau_0$, $\Gamma_5 = \eta_3 \sigma_2 \tau_0$ and $\Gamma_6 = \eta_1 \sigma_0 \tau_0$. The set of Pauli matrices η operate on the sublattice degrees of freedom. Then, its NH version $H_{\text{NH}}(\mathbf{k})$ [Eq. (5)] supports eight zero-energy corner modes. All the results are shown in Fig. 4.

NH Topological semimetals. By stacking NH TIs, one can realize NH TSMs depending on Δ_1/B and t_s/B . They are also devoid of any NH skin effect and support gapless boundary modes when $|\alpha| < 1$. Here, we discuss some key examples. NH Su-Schrieffer-Heeger insulators, stacked in the y direction, can produce a NH Dirac semimetal in $d = 2$ (like graphene) that supports

Fermi arcs between two Dirac points, located along the k_y axis. By continuing such stacking in the z direction, we can find a NH nodal-loop semimetal, supporting drum-head surface states on the (k_y, k_z) planes. By the same token, stacked (in the z direction) NH Chern insulators yield a three-dimensional NH Weyl semimetal with surface Fermi arcs occupying the (k_z, x) and (k_z, y) planes in between two Weyl nodes along k_z . And stacking of NH second-order TIs produces NH higher-order Dirac semimetal in $d = 3$, featuring only z directional hinge modes localized within the Dirac nodes on the k_z axis. These outcomes for specific choices of Δ_1/B and t_s/B are shown in Fig. 5. Notice that topological boundary modes from opposite ends of the system get connected via bulk nodal points or loops in all the NH TSMs, where the localization length of the zero-modes of the underlying NH TIs diverges. Weak TIs obtained in the same way are also devoid of any NH skin effect and accommodate topological boundary modes, which, however, occupy the entire Brillouin zone along the stacking direction(s).

Discussion & outlook. Here we unfold a general principle of constructing NH insulating and nodal topological phases in any dimension that are always devoid of NH skin effects. In the topological regime, they showcase the BBC in terms of either the right or left zero-energy eigenmodes, when all the eigenvalues of the NH operators are purely real. The systems become trivial when these eigenvalues are complex. See Figs. 1-5. In order to numerically ensure the bi-orthonormality condition $\langle \Psi_i^L | \Psi_j^R \rangle = \delta_{ij}$ between the real space left (L) and right (R) eigenmodes of $H_{\text{NH}}(\mathbf{k})$ with eigenvalues E_i and E_j , respectively, we sometime have to add an extremely small amount of random charge disorder ($\sim 10^{-4} - 10^{-6}$). Our construction can be immediately generalized for NH crystalline topological phases, as in the Hermitian limit their universal Bloch Hamiltonian takes the form of $H_{\text{Her}}(\mathbf{k})$, however, involving longer-range hopping processes (beyond NN), allowed crystal symmetries [89–91]. In the future, it will be worthwhile extending this construction for NH topological superconductors. The quantum critical points separating NH topological and trivial insulators are described by NH Dirac or Weyl fermions. Stability of such NH critical points against electronic interactions [92, 93] and disorder is still in its infancy.

Simplicity of our construction for the NH topological operators should make them realizable on multiple platforms, as $H_{\text{NH}}(\mathbf{k})$ involves only NN hopping amplitudes and on-site staggered potential [Eq. (5)]. For example, electronic designer materials [94–98] and optical lattices constitute a promising quantum platform where these operators and the resulting NH topological phases can be realized. In the former system, a hopping imbalance (yielding non-Hermiticity) can be engineered by placing electronic valves along the NN bonds, permitting unidirectional electronic hopping, however, set at different operational voltages in the opposite directions. On op-

tical lattices, it can be achieved with different laser intensities in the opposite directions along the NN bonds, as recently has been demonstrated on one-dimensional chains [37]. Topological modes in these setups can be detected by the standard scanning tunneling spectroscopy since the proposed NH topological phases are always devoid of the NH skin effect.

Classical metamaterials, such as photonic and mechanical lattices, as well as topoelectric circuits, constitute yet another set of viable avenues along which the predicted NH topology can be experimentally displayed. On all these platforms, tunable NN hopping can be implemented and a plethora of NH topological phases with NH skin effects has already been realized [38–50]. Lack of the NH skin effect associated with all our NH operators should allow the detection of classical topological modes in these systems using well-developed tools (already applied for Hermitian topological systems), such as the two-point pump probe spectroscopy (on photonic lattices), mechanical (on mechanical lattices) and electrical (on topoelectric circuits) impedance. Current discussion should therefore stimulate a new surge of experimental works exploring the BBC in skin effect-free NH systems in terms of solely the left and right topological eigenmodes.

Acknowledgments. D.J.S. was supported by NSF CAREER Grant No. DMR- 2238679 of B.R. and S.K.D. was supported by the Startup Grant of B.R. from Lehigh University.

* Equal contributors

† Corresponding author: bitan.roy@lehigh.edu

- [1] M. Z. Hasan and C. L. Kane, Colloquium: Topological insulators, *Rev. Mod. Phys.* **82**, 3045 (2010).
- [2] X.-L. Qi and S.-C. Zhang, Topological insulators and superconductors, *Rev. Mod. Phys.* **83**, 1057 (2011).
- [3] C.-K. Chiu, J. C. Y. Teo, A. P. Schnyder, and S. Ryu, Classification of topological quantum matter with symmetries, *Rev. Mod. Phys.* **88**, 035005 (2016).
- [4] A. Bansil, H. Lin, and T. Das, Colloquium: Topological band theory, *Rev. Mod. Phys.* **88**, 021004 (2016).
- [5] C. L. Kane and E. J. Mele, Z_2 Topological Order and the Quantum Spin Hall Effect, *Phys. Rev. Lett.* **95**, 146802 (2005).
- [6] B. A. Bernevig, T. L. Hughes, and S.-C. Zhang, Quantum Spin Hall Effect and Topological Phase Transition in HgTe Quantum Wells, *Science* **314**, 1757 (2006).
- [7] L. Fu and C. L. Kane, Topological insulators with inversion symmetry, *Phys. Rev. B* **76**, 045302 (2007).
- [8] J. E. Moore and L. Balents, Topological invariants of time-reversal-invariant band structures, *Phys. Rev. B* **75**, 121306 (2007).
- [9] R. Roy, Topological phases and the quantum spin Hall effect in three dimensions, *Phys. Rev. B* **79**, 195322 (2009).
- [10] C.-X. Liu, X.-L. Qi, H. Zhang, X. Dai, Z. Fang, and S.-C. Zhang, Model Hamiltonian for topological insulators, *Phys. Rev. B* **82**, 045122 (2010).

- [11] S. Ryu, A. P. Schnyder, A. Furusaki, and A. W. W. Ludwig, Topological insulators and superconductors: tenfold way and dimensional hierarchy, *New J. Phys.* **12**, 065010 (2010).
- [12] S. K. Das and B. Roy, Hybrid symmetry class topological insulators, [arXiv:2305.16313](https://arxiv.org/abs/2305.16313).
- [13] A. H. Castro Neto, F. Guinea, N. M. R. Peres, K. S. Novoselov, and A. K. Geim, The electronic properties of graphene, *Rev. Mod. Phys.* **81**, 109 (2009).
- [14] N. P. Armitage, E. J. Mele, and A. Vishwanath, Weyl and Dirac semimetals in three-dimensional solids, *Rev. Mod. Phys.* **90**, 015001 (2018).
- [15] X. Wan, A. M. Turner, A. Vishwanath, and S. Y. Savrasov, Topological semimetal and Fermi-arc surface states in the electronic structure of pyrochlore iridates, *Phys. Rev. B* **83**, 205101 (2011).
- [16] A. A. Burkov and L. Balents, Weyl Semimetal in a Topological Insulator Multilayer, *Phys. Rev. Lett.* **107**, 127205 (2011).
- [17] B.-J. Yang and N. Nagaosa, Classification of stable three-dimensional Dirac semimetals with nontrivial topology, *Nat. Commun.* **5**, 4898 (2014).
- [18] B. Bradlyn, J. Cano, Z. Wang, M. G. Vergniory, C. Felser, R. J. Cava, and B. A. Bernevig, Beyond Dirac and Weyl fermions: Unconventional quasiparticles in conventional crystals, *Science* **353**, aaf5037 (2016).
- [19] G. E. Volovik, *The Universe in a Helium Droplet* (Oxford University Press, Oxford, UK, 2009).
- [20] N. Read and D. Green, Paired states of fermions in two dimensions with breaking of parity and time-reversal symmetries and the fractional quantum Hall effect, *Phys. Rev. B* **61**, 10267 (2000).
- [21] A. Kitaev, Periodic table for topological insulators and superconductors, *AIP Conf. Proc.* **1134**, 22 (2009).
- [22] M. Sato and Y. Ando, Topological superconductors: a review, *Rep. Prog. Phys.* **80**, 076501 (2017).
- [23] Y. Ando and L. Fu, Topological Crystalline Insulators and Topological Superconductors: From Concepts to Materials, *Annu. Rev. Condens. Matter Phys.* **6**, 361 (2015).
- [24] W. A. Benalcazar, B. A. Bernevig, and T. L. Hughes, Quantized electric multipole insulators, *Science* **357**, 61 (2017).
- [25] W. A. Benalcazar, B. A. Bernevig, and T. L. Hughes, Electric multipole moments, topological multipole moment pumping, and chiral hinge states in crystalline insulators, *Phys. Rev. B* **96**, 245115 (2017).
- [26] Z. Song, Z. Fang, and C. Fang, $(d - 2)$ -Dimensional Edge States of Rotation Symmetry Protected Topological States, *Phys. Rev. Lett.* **119**, 246402 (2017).
- [27] J. Langbehn, Y. Peng, L. Trifunovic, F. von Oppen, and P. W. Brouwer, Reflection-Symmetric Second-Order Topological Insulators and Superconductors, *Phys. Rev. Lett.* **119**, 246401 (2017).
- [28] F. Schindler, A. M. Cook, M. G. Vergniory, Z. Wang, S. S. P. Parkin, B. A. Bernevig, and T. Neupert, Higher-order topological insulators, *Sci. Adv.* **4**, eaat0346 (2018).
- [29] E. Khalaf, Higher-order topological insulators and superconductors protected by inversion symmetry, *Phys. Rev. B* **97**, 205136 (2018).
- [30] C.-H. Hsu, P. Stano, J. Klinovaja, and D. Loss, Majorana Kramers Pairs in Higher-Order Topological Insulators, *Phys. Rev. Lett.* **121**, 196801 (2018).
- [31] A. Matsugatani and H. Watanabe, Connecting higher-order topological insulators to lower-dimensional topological insulators, *Phys. Rev. B* **98**, 205129 (2018).
- [32] Z. Wang, B. J. Wieder, J. Li, B. Yan, and B. A. Bernevig, Higher-Order Topology, Monopole Nodal Lines, and the Origin of Large Fermi Arcs in Transition Metal Dichalcogenides XTe_2 ($X = Mo, W$), *Phys. Rev. Lett.* **123**, 186401 (2019).
- [33] L. Trifunovic and P. W. Brouwer, Higher-Order Bulk-Boundary Correspondence for Topological Crystalline Phases, *Phys. Rev. X* **9**, 011012 (2019).
- [34] D. Călugăru, V. Juričić, and B. Roy, Higher-order topological phases: A general principle of construction, *Phys. Rev. B* **99**, 041301 (2019).
- [35] B. Roy, Antiunitary symmetry protected higher-order topological phases, *Phys. Rev. Res.* **1**, 032048 (2019).
- [36] T. Nag, V. Juričić, and B. Roy, Hierarchy of higher-order Floquet topological phases in three dimensions, *Phys. Rev. B* **103**, 115308 (2021).
- [37] Q. Liang, D. Xie, Z. Dong, H. Li, H. Li, B. Gadway, W. Yi, and B. Yan, Dynamic signatures of non-hermitian skin effect and topology in ultracold atoms, *Phys. Rev. Lett.* **129**, 070401 (2022).
- [38] B. Zhen, C. W. Hsu, Y. Igarashi, L. Lu, I. Kaminer, A. Pick, S.-L. Chua, J. D. Joannopoulos, and M. Soljačić, Spawning rings of exceptional points out of Dirac cones, *Nature (London)* **525**, 354 (2015).
- [39] S. Weimann, M. Kremer, Y. Plotnik, Y. Lumer, S. Nolte, K. G. Makris, M. Segev, M. C. Rechtsman, and A. Szameit, Topologically protected bound states in photonic parity-time-symmetric crystals, *Nat. Mater.* **16**, 433 (2016).
- [40] H. Zhou, C. Peng, Y. Yoon, C. W. Hsu, K. A. Nelson, L. Fu, J. D. Joannopoulos, M. Soljačić, and B. Zhen, Observation of bulk Fermi arc and polarization half charge from paired exceptional points, *Science* **359**, 1009 (2018).
- [41] A. Cerjan, S. Huang, M. Wang, K. P. Chen, Y. Chong, and M. C. Rechtsman, Experimental realization of a Weyl exceptional ring, *Nat. Photon.* **13**, 623 (2019).
- [42] H. Zhao, X. Qiao, T. Wu, B. Midya, S. Longhi, and L. Feng, Non-Hermitian topological light steering, *Science* **365**, 1163 (2019).
- [43] M. Kremer, T. Biesenthal, L. J. Maczewsky, M. Heinrich, R. Thomale, and A. Szameit, Demonstration of a two-dimensional \mathcal{PT} -symmetric crystal, *Nat. Commun.* **10**, 435 (2019).
- [44] C. Shi, M. Dubois, Y. Chen, L. Cheng, H. Ramezani, Y. Wang, and X. Zhang, Accessing the exceptional points of parity-time symmetric acoustics, *Nat. Commun.* **7**, 11110 (2016).
- [45] W. Zhu, X. Fang, D. Li, Y. Sun, Y. Li, Y. Jing, and H. Chen, Simultaneous Observation of a Topological Edge State and Exceptional Point in an Open and Non-Hermitian Acoustic System, *Phys. Rev. Lett.* **121**, 124501 (2018).
- [46] M. Brandenbourger, X. Locsin, E. Lerner, and C. Coulais, Non-reciprocal robotic metamaterials, *Nat. Commun.* **10**, 4608 (2019).
- [47] A. Ghatak, M. Brandenbourger, J. van Wezel, and C. Coulais, Observation of non-Hermitian topology and its bulk-edge correspondence in an active mechanical metamaterial, *Proc. Natl. Acad. Sci. U.S.A.* **117**, 29561 (2020).
- [48] T. Hofmann, T. Helbig, F. Schindler, N. Salgo, M. Brzezińska, M. Greiter, T. Kiessling, D. Wolf, A. Vollhardt, A. Kabaši, C. H. Lee, A. Bilušić, R. Thomale, and

- T. Neupert, Reciprocal skin effect and its realization in a topolectrical circuit, *Phys. Rev. Res.* **2**, 023265 (2020).
- [49] L. Li, C. H. Lee, S. Mu, and J. Gong, Critical non-Hermitian skin effect, *Nat. Commun.* **11**, 5491 (2020).
- [50] A. Stegmaier, S. Imhof, T. Helbig, T. Hofmann, C. H. Lee, M. Kremer, A. Fritzsche, T. Feichtner, S. Klemmt, S. Höfling, I. Boettcher, I. C. Fulga, L. Ma, O. G. Schmidt, M. Greiter, T. Kiessling, A. Szameit, and R. Thomale, Topological Defect Engineering and \mathcal{PT} Symmetry in Non-Hermitian Electrical Circuits, *Phys. Rev. Lett.* **126**, 215302 (2021).
- [51] L. E. F. F. Torres, Perspective on topological states of non-Hermitian lattices, *J. Phys. Mater.* **3**, 014002 (2019).
- [52] A. Ghatak and T. Das, New topological invariants in non-Hermitian systems, *J. Phys.: Condens. Matter* **31**, 263001 (2019).
- [53] E. J. Bergholtz, J. C. Budich, and F. K. Kunst, Exceptional topology of non-Hermitian systems, *Rev. Mod. Phys.* **93**, 015005 (2021).
- [54] K. Esaki, M. Sato, K. Hasebe, and M. Kohmoto, Edge states and topological phases in non-Hermitian systems, *Phys. Rev. B* **84**, 205128 (2011).
- [55] S.-D. Liang and G.-Y. Huang, Topological invariance and global Berry phase in non-Hermitian systems, *Phys. Rev. A* **87**, 012118 (2013).
- [56] S. Yao and Z. Wang, Edge States and Topological Invariants of Non-Hermitian Systems, *Phys. Rev. Lett.* **121**, 086803 (2018).
- [57] S. Yao, F. Song, and Z. Wang, Non-Hermitian Chern Bands, *Phys. Rev. Lett.* **121**, 136802 (2018).
- [58] Z. Gong, Y. Ashida, K. Kawabata, K. Takasan, S. Higashikawa, and M. Ueda, Topological Phases of Non-Hermitian Systems, *Phys. Rev. X* **8**, 031079 (2018).
- [59] K. Kawabata, K. Shiozaki, and M. Ueda, Anomalous helical edge states in a non-Hermitian Chern insulator, *Phys. Rev. B* **98**, 165148 (2018).
- [60] H. Shen, B. Zhen, and L. Fu, Topological Band Theory for Non-Hermitian Hamiltonians, *Phys. Rev. Lett.* **120**, 146402 (2018).
- [61] F. K. Kunst, E. Edvardsson, J. C. Budich, and E. J. Bergholtz, Biorthogonal Bulk-Boundary Correspondence in Non-Hermitian Systems, *Phys. Rev. Lett.* **121**, 026808 (2018).
- [62] K. Kawabata, S. Higashikawa, Z. Gong, Y. Ashida, and M. Ueda, Topological unification of time-reversal and particle-hole symmetries in non-Hermitian physics, *Nat. Commun.* **10**, 297 (2019).
- [63] H. Zhou and J. Y. Lee, Periodic table for topological bands with non-Hermitian symmetries, *Phys. Rev. B* **99**, 235112 (2019).
- [64] K. Yokomizo and S. Murakami, Non-Bloch Band Theory of Non-Hermitian Systems, *Phys. Rev. Lett.* **123**, 066404 (2019).
- [65] K. Kawabata, K. Shiozaki, M. Ueda, and M. Sato, Symmetry and topology in non-hermitian physics, *Phys. Rev. X* **9**, 041015 (2019).
- [66] C. H. Lee and R. Thomale, Anatomy of skin modes and topology in non-Hermitian systems, *Phys. Rev. B* **99**, 201103 (2019).
- [67] N. Okuma, K. Kawabata, K. Shiozaki, and M. Sato, Topological Origin of Non-Hermitian Skin Effects, *Phys. Rev. Lett.* **124**, 086801 (2020).
- [68] C. Scheibner, W. T. M. Irvine, and V. Vitelli, Non-Hermitian Band Topology and Skin Modes in Active Elastic Media, *Phys. Rev. Lett.* **125**, 118001 (2020).
- [69] L. Xiao, T. Deng, K. Wang, G. Zhu, Z. Wang, W. Yi, and P. Xue, Non-Hermitian bulk–boundary correspondence in quantum dynamics, *Nat. Phys.* **16**, 761 (2020).
- [70] K. Zhang, Z. Yang, and C. Fang, Correspondence between Winding Numbers and Skin Modes in Non-Hermitian Systems, *Phys. Rev. Lett.* **125**, 126402 (2020).
- [71] D. S. Borgnia, A. J. Kruchkov, and R.-J. Slager, Non-Hermitian Boundary Modes and Topology, *Phys. Rev. Lett.* **124**, 056802 (2020).
- [72] H. C. Wu, L. Jin, and Z. Song, Nontrivial topological phase with a zero Chern number, *Phys. Rev. B* **102**, 035145 (2020).
- [73] A. Altland, M. Fleischhauer, and S. Diehl, Symmetry classes of open fermionic quantum matter, *Phys. Rev. X* **11**, 021037 (2021).
- [74] X.-Q. Sun, P. Zhu, and T. L. Hughes, Geometric Response and Disclination-Induced Skin Effects in Non-Hermitian Systems, *Phys. Rev. Lett.* **127**, 066401 (2021).
- [75] W. Zhu, W. X. Teo, L. Li, and J. Gong, Delocalization of topological edge states, *Phys. Rev. B* **103**, 195414 (2021).
- [76] S. Manna and B. Roy, Inner skin effects on non-Hermitian topological fractals, *Commun. Phys.* **6**, 10 (2023).
- [77] W. P. Su, J. R. Schrieffer, and A. J. Heeger, Solitons in Polyacetylene, *Phys. Rev. Lett.* **42**, 1698 (1979).
- [78] W. P. Su, J. R. Schrieffer, and A. J. Heeger, Soliton excitations in polyacetylene, *Phys. Rev. B* **22**, 2099 (1980).
- [79] A. J. Heeger, S. Kivelson, J. R. Schrieffer, and W. P. Su, Solitons in conducting polymers, *Rev. Mod. Phys.* **60**, 781 (1988).
- [80] X.-L. Qi, Y.-S. Wu, and S.-C. Zhang, Topological quantization of the spin Hall effect in two-dimensional paramagnetic semiconductors, *Phys. Rev. B* **74**, 085308 (2006).
- [81] R.-J. Slager, V. Juričić, and B. Roy, Dissolution of topological Fermi arcs in a dirty Weyl semimetal, *Phys. Rev. B* **96**, 201401 (2017).
- [82] A. A. Burkov, M. D. Hook, and L. Balents, Topological nodal semimetals, *Phys. Rev. B* **84**, 235126 (2011).
- [83] T. T. Heikkilä and G. E. Volovik, Dimensional crossover in topological matter: Evolution of the multiple Dirac point in the layered system to the flat band on the surface, *JETP Lett.* **93**, 59 (2011).
- [84] B. Roy, Interacting nodal-line semimetal: Proximity effect and spontaneous symmetry breaking, *Phys. Rev. B* **96**, 041113 (2017).
- [85] M. Lin and T. L. Hughes, Topological quadrupolar semimetals, *Phys. Rev. B* **98**, 241103 (2018).
- [86] A. L. Szabó, R. Moessner, and B. Roy, Strain-engineered higher-order topological phases for spin- $\frac{3}{2}$ Luttinger fermions, *Phys. Rev. B* **101**, 121301 (2020).
- [87] A. C. Tyner, S. Sur, D. Puggioni, J. M. Rondinelli, and P. Goswami, Topology of three-dimensional Dirac semimetals and quantum spin Hall systems without gapless edge modes, *Phys. Rev. Res.* **5**, L012019 (2023).
- [88] B. Roy and V. Juričić, Mixed-parity octupolar pairing and corner Majorana modes in three dimensions, *Phys. Rev. B* **104**, L180503 (2021).
- [89] L. Fu, Topological Crystalline Insulators, *Phys. Rev. Lett.* **106**, 106802 (2011).
- [90] R.-J. Slager, A. Mesaros, V. Juričić, and J. Zaanen, The space group classification of topological band-insulators, *Nat. Phys.* **9**, 98 (2012).
- [91] K. Shiozaki and M. Sato, Topology of crystalline insulators and superconductors, *Phys. Rev. B* **90**, 165114

- (2014).
- [92] V. Juricic and B. Roy, Yukawa-Lorentz Symmetry in Non-Hermitian Dirac Materials, [arXiv:2308.16907](#).
- [93] S. A. Murshed and B. Roy, Quantum Electrodynamics of Non-Hermitian Dirac Fermions, [arXiv:2309.07916](#).
- [94] K. K. Gomes, W. Mar, W. Ko, F. Guinea, and H. C. Manoharan, Designer Dirac fermions and topological phases in molecular graphene, *Nature (London)* **483**, 306 (2012).
- [95] M. Polini, F. Guinea, M. Lewenstein, H. C. Manoharan, and V. Pellegrini, Artificial honeycomb lattices for electrons, atoms and photons, *Nature Nanotech* **8**, 625 (2013).
- [96] L. C. Collins, T. G. Witte, R. Silverman, D. B. Green, and K. K. Gomes, Imaging quasiperiodic electronic states in a synthetic Penrose tiling, *Nat. Commun.* **8**, 15961 (2017).
- [97] S. N. Kempkes, M. R. Slot, S. E. Freeney, S. J. M. Zevenhuizen, D. Vanmaekelbergh, I. Swart, and C. M. Smith, Design and characterization of electrons in a fractal geometry, *Nat. Phys.* **15**, 127 (2019).
- [98] S. N. Kempkes, M. R. Slot, J. J. van den Broeke, P. Capiod, W. A. Benalcazar, D. Vanmaekelbergh, D. Bercioux, I. Swart, and C. Morais Smith, Robust zero-energy modes in an electronic higher-order topological insulator, *Nat. Mater.* **18**, 1292 (2019).